



C:10

Hydrography Committee
Sess. Computers in
Fishery Research

FOLLOW-UP AND PREDICTION OF UPWELLING IN THE IBERIAN PENINSULA WEST COAST USING METEOROLOGIC PARAMETERS, EKMAN FLUX AND SATELLITE REMOTE SENSIG

J. Torres*, J. Triñanes, A. Tobar**, C. Hernández***

**University of Santiago.
15706 Santiago de Compostela. Spain.**

*** Applied Physics Department.**

**** Electronics and Computer Sciences.**

**University of La Laguna
Santa Cruz de Tenerife. Spain**

*****Fundamental and Experimental Physics Department.**

ABSTRACT

The upwelling has been showed like most important physical event that gives basic nutrients for developing marine life .The parameter that give us the better idea about the amount of upwelling water is Ekman flux ,that is obtained from geostrophic wind in the area of study. Using the remote infrared sensors in satellite we are able to test the appearance of this kind of events.

One system that allow us to study the temporal evolution of geostrophic winds and calculate the Ekman flux for predicting and following-up of upwelling has been developed. We obtain the wind from isobaric maps sent by METEOSAT satellite ,with which we compute Ekman flux. We have made a temporal averaged study of this parameters and developed threedimensional graphics representation that allow us to integrate the isobaric information , chromatically quantifier, with the information coming from the geostrophic winds and to make a geographic registration. With all this information we have made the prediction and following-up of the ocean event and test the results with thermal imagery.

A paper presented at the 81st Statutory Meeting of the International Council for the Exploration of the Sea (ICES). Dublin, Ireland. 23 September-1 October, 1993

INTRODUCTION

We have related atmospheric events to the appearance of sea areas rich in phosphates and nutrients, which impulse the development of phytoplankton and with it, that of the marine species which lie within the trophic chain and which are a basis of human feeding.

In these areas, an increase in nutrients is produced along the shore by the upwelling of waters from depths of 100 to 200 metres to the surface. They are detected by means of satellites because this rise or "upwelling" occurs at a lower temperature than that of the surrounding water, approximately two or three degrees lower, which may even cause the formation of fog in the area of upwelling.

This fact has been revealed as the most important physical phenomenon which provides the chemical fertilizers, nitrates and phosphates needed in the biological development of fishing resources.

According to Maeda and Kishimoto (1970), the main areas of shore upwelling are located in the East margin of the large anticyclonic whirlwinds of sea circulation, on the West continental shores, between latitudes 10 and 50 of both hemispheres. It is no coincidence that the most important fishing banks in the world appear in these spots of the planets.

-The first explanation for fishing upwelling was given by Ekman in 1905.

Wind exerts a definite deforming effort over the sea surface, in the same direction in which it blows. Immediately, and owing to the rotation of the Earth, a force acts over the bodies which are in movement relative to the Earth. This force, called Coriolis force, follows the normal direction of the movement and causes the wind to move to the right of the direction of the movement in the Northern hemisphere and to its left in the Southern hemisphere.

This effect is gradually transmitted from the wind to the surface of the water, which is moved towards the right in the superficial layers of the Northern hemisphere. When the wind in this hemisphere is of a Northern component and parallel to the coast, a superficial current is produced offshore, and vacuum is formed being filled by the deeper, colder and more nutrient waters.
(see Figure 1 (upwelling))

In the waters off the West coast of the Iberian Peninsula, under the influence of high pressures, North winds favouring upwelling are generated between the months of April and September; during the rest of the year, southwest winds are predominant, producing the contrary effect: piling up of water which comes from the high seas towards the coast or "downwelling".

According to Blanton, winds favourable for "upwelling" prevail in Galicia from April to October. The same is shown by R. Molina with data gathered from 1931-60.

The magnitude of Ekman's component in the deep seas is considered to be an indicator of the amount of florid water. In order to calculate this index, we will first calculate the geostrophic winds by means of pressure maps.

According to Fizua, the average season of upwelling is from July to September on the Portuguese coast. By using average data of 29 years, he also points out a correlation between the Northern component of the wind, the appearance of upwelling and the highest catches of sardine, the time difference between cause-effect being of one month for upwelling and of three months for the highest catches. Blanton also relates Ekman's high transport indexes with the development of mussels in the Galician estuaries, for which he uses the "upwelling" index and the index of mussel development between the years 1969-1985.

EQUATIONS:

The equation for the movement of winds relative to land in polar coordinates is the following:

$$\frac{dV}{dt} = -\frac{1}{\rho} \nabla p - g - 2\Omega \times V + F_r \quad (1)$$

The values to the right of the equality in equation (1) are due to the accelerations of the pressure gradient force, the gravity ($g = g_{in} - \Omega \times (\Omega \times a)$) gravitation minus the earth's centripid acceleration, Coriolis force and friction respectively.

Owing to the fact that the Earth is spheric, the individual components of equation (1) will be as follows:

$$2\Omega w \cos \phi + \frac{\delta u}{dt} + \left(-\frac{uv \tan \phi}{a} + \frac{uw}{a} \right) - 2\Omega v \sin \phi = -\frac{1}{\rho} \frac{dp}{dx} + F_x \quad (2)$$

$$\frac{dv}{dt} + \left(\frac{u^2 \tan \phi}{a} + \frac{vw}{a} \right) + 2\Omega u \sin \phi = -\frac{1}{\rho} \frac{dp}{dy} + F_y \quad (3)$$

$$\frac{dw}{dt} + \left(-\frac{u^2 + v^2}{a} \right) - 2\Omega u \cos \phi = -\frac{1}{\rho} \frac{dp}{dz} - g + F_z \quad (4)$$

and the continuity equation is realized as:

$$\frac{1}{\rho} \cdot \frac{dp}{dt} + \left(-\frac{v \tan \phi}{a} + \frac{2w}{a} \right) + \frac{\delta u}{\delta x} + \frac{\delta v}{\delta y} + \frac{\delta w}{\delta z} = 0 \quad (5)$$

Here (X,y,z) and (u,v,w) represent the East, North East and the ascendent coordinates and the term between brakets is due to the curvature of the Earth.

APPROXIMATION OF EQUATIONS:

The equations do not generally have analytic solutions. For this reason, it is necessary to simplify them in order to consider a particular phenomenon. One possible way would be to reduce the higher order members in each equation.

The terms found between brakets in the equations (2,3,4 y 5) are due to the curvature of the Earth and are important in movements at a global scale. For movements at a local scale they can be ignored. Using the information in the table (1):

Atmospheric Circulation Systems

TABLE 1.1 Typical Magnitudes for Different Motion Scales

	Extratropical Low	Hurricane ↓	Thunderstorm ↓
Time (seconds)	10 ⁵	10 ⁵	10 ³
Length (meters)	10 ⁶	10 ⁵	10 ⁴
Height (meters)	10 ⁴	10 ⁴	10 ⁴
Velocity (meters per second)	10 ¹	3 × 10 ¹	10 ¹
Vertical velocity (meters per second)	10 ⁻²	10 ⁻¹	10 ¹
Horizontal pressure variation (pascals)	10 ²	3 × 10 ²	10 ¹

in the equation (5) we get that in a typical extratropical cyclon

$$u \frac{\delta u}{\delta x} \approx \frac{(10)(10)}{10^6} = 10^{-4} \text{ m}^2 \text{ s}^{-1} \quad (6)$$

whereas in medium latitudes where $\tan(\phi) = O(1)$

$$\frac{uv \tan \phi}{a} \approx 10^{-5} \text{ m}^2 \text{ s}^{-1} \quad (7)$$

for those movements the parameter of the Coriolis force, $f = 2\Omega \sin \phi$, may be taken as a constant or as a lineal function of the latitude $f = f_0 \Omega + \beta y$

On the other hand, in the majority of the high scale movements of the Earth, vertical acceleration is important when it is compared to gravity acceleration. Thus, for example, in equation (4) we obtain:

$$\frac{\delta w}{\delta t} \approx u \frac{\delta w}{\delta x} \approx 10^{-7} \ll 10^1 \approx g \approx \frac{1}{\rho} \frac{\delta p}{\delta z} \quad (8)$$

Moreover, to obtain a high precision level, the vertical movement equation is reduced to a state of hydrostatic balance.

$$0 = -\frac{1}{\rho} \frac{\delta p}{\delta z} - g \quad (9)$$

for a movement of synoptic scale.

These movements are almost hydrostatic and allow us to represent them almost in Lagrangian presicion coordenates rather than in ordinary Cartesian ones (x,y,z). Under such conditions the equality equation is reduced to:

$$\left. \frac{\delta u}{\delta x} \right|_p + \left. \frac{\delta v}{\delta y} \right|_p + \frac{\delta w}{\delta z} = 0 \quad (10)$$

where $w = dp/dt$ is analogous with vertical velocity. $\Omega = -\rho g w$

For a first approximation the acceleration terms may be ignored in horizontal movement equations, which are reduced to the so called equations of geostrophic wind.:

$$\begin{aligned} v &= \left. \frac{g}{f} \frac{\delta z}{\delta x} \right|_p = \frac{1}{\rho f} \left. \frac{\delta p}{\delta x} \right|_z \\ u &= -\left. \frac{g}{f} \frac{\delta z}{\delta x} \right|_p = -\frac{1}{\rho f} \left. \frac{\delta p}{\delta x} \right|_z \end{aligned} \quad (11)(12)$$

In order to calculate the index of upwelling, following Bakun's methodology, it is necessary to know daily winds, and owing to the fact that there are no real measures for them in the sea, it is necessary to resort to geostrophic wind, which is an approximation to real wind, derived from an atmospheric pressure difference in a cell where the point being considered is the centre.

Once the speed and direction of the wind have been obtained, the deforming effort

that it exerts over the sea surface is calculated. This produces a superficial movement in a perpendicular sense and towards the right of the direction of the wind, and the vacuum is filled by the same subsuperficial water.

In order to obtain the speed and the direction of the wind produced by the difference of pressures found in the medium point of the opposite sides of the cell in question, it is necessary to measure the pressures corresponding to each point separated at a distance δx and δy .

The geostrophic equations which give us the wind component are:

$$U = -\alpha * f^{-1} * \left(\frac{\delta p}{\delta y} \right) \text{ comp. Este}$$

$$V = -\alpha * f^{-1} * \left(\frac{\delta p}{\delta x} \right) \text{ comp. Norte} \quad (13)(14)$$

where α is the specific volume of air and f is the Coriolis parameter,

$$\alpha = R \quad (15)$$

Owing to the friction existing over the surface, the geostrophic values of winds thus obtained have to be turned 15 grades towards the right and have to be applied a 0.7 decrease factor, and consequently, the deforming effort over the surface is now:

$$T_x = \rho * C_d (U^2 + V^2)^{1/2} * U$$

$$T_y = \rho * C_d (U^2 + V^2)^{1/2} * V \quad (16)(17)$$

This deforming effect over the surface, generates a current which flows to the right of the direction of the wind in the Northern hemisphere and as we have already mentioned, it is called Ekman's current. In this case, it is the north winds that originate the upwelling, because when a superficial current is induced towards the west, it has to be replaced by deeper waters. This movement has the following equations when there is a lack of pressure gradient and the friction is being considered:

$$\begin{aligned} \rho * \phi * V_E + \delta \tau_x / \delta x &= 0 \\ \rho * \phi * U_E + \delta \tau_y / \delta y &= 0 \end{aligned} \quad (18)(19)$$

ρ water density
 τ_{xy} wind force on sea surface in xy direction

U_E, V_E components of Ekman velocity

$$\begin{aligned} \rho * f * V_E * \delta z &= -\delta \tau_x \\ \rho * f * U_E * \delta z &= \delta \tau_y \end{aligned} \quad (20)(21)$$

where $\rho * V_E * \delta z$ is the mass that flows in the direction and per second through an area of $1m \times 1m$ in the xy plane. The same applies to $\rho * U_E * \delta z$ with respect to the x axis. If Z is the depth where the value of speed is zero with respect to the superficial, the integrals between zero and z in equations (20 y 21) give us the total of the mass transported by the current induced by the wind.

Using M_{xE} and M_{yE} to represent the transports in the directions x, y already mentioned, we obtain:

$$f * M_{yE} = -\tau_x \quad f * M_{xE} = \tau_y \quad (22)$$

and if we transform it into volume

$$f * Q_{yE} = -\alpha * \tau_x \quad f * Q_{xE} = \alpha * \tau_y \quad (23)$$

where Q is the volume of transported water and

$$\alpha = 1/\rho \quad (24)$$

Thus, the amount of water displaced by Ekman's effect along the path parallel to the coast, in a perpendicular way with respect to it, which is no other thing than the index of upwelling is:

$$I_w = -\tau_y / (f * \rho) \text{ [m}^3 \text{ / seg]} \quad (25)$$

We generate average pressure maps which correspond to a period of time considered for our study.

We can calculate the average of the geostrophic winds and thus we can know the winds which are dominant both in direction and speed in any point in the map. We represent the pressure map in tridimensional perspective. The anticyclons correspond to the peaks and the storms to the valleys. We also get a projection of the isobars corresponding to that pressure map over the geographic one.

We make a vectorial representation of the winds for each point in the map separated by 2 degrees from all the others, where each vector has the direction of the geostrophic wind for that point and the map of pressures being considered, and which has a module proportional to the speed of the wind calculated for that point.

In this way we can foresee the appearance of upwelling at some point in the map because what we are representing is the predominant winds in the period of time in consideration.

We can also calculate the winds and Ekman's index daily during a long period of time in consideration. In this case we make the calculations for a position given initially by its geographic coordinates. Now, the results of such processes will represent the daily variations in the wind (direction and speed) and Ekman's index.

Thus, we can follow what is going on with the wind in a precise place during a whole month, something that will prove of great importance when it comes to the prediction of the appearance of upwelling.

RESULTS

We have introduced the isobar maps corresponding to a whole month from July 13th to August 12th 1991, where we will study the average maps per week, calculating the geostrophic winds for each of them. Finally, during this month we will carry out a study of the variations of direction, speed and Ekman's index for the three points located along the Iberian Coast.

WEEK FROM JULY 13th TO 19th

A strong anticyclone with a center in parallel 35N meridian 40W is observed in the map of pressures. It exerts its influence from Great Britain up to all the Mediterranean. A storm is located in the Scandinavian Peninsula.

As to the geostrophic winds, it is observed that they flow parallel to the French and Iberian coasts, being salient towards the ocean at the Gibraltar Strait from the Mediterranean. Winds parallel to the Coast of Great Britain appear in the English Channel.

WEEK FROM JULY 20th TO 27th

The strong anticyclone persists though somewhat less intense this week. W to 30W in the 60N parallel. Another storm seems to appear in the South of Libyan and another front with low pressures is approaching from the West of Europe.

As to the winds, we can see a slight variation with respect to the previous week. Now the winds in front of the Cantabric coast are parallel to it with a direction towards the East. In Great Britain, winds of South component parallel to the coast and on the French Coast of the "Viscaya Golf" the W component winds are entering the Coast. On the Galician coast there are also East component winds this week, while on the South half of the Iberian coast in the Atlantic, the predominant winds are of a North component, favouring the appearance of upwelling in the area. On the Mediterranean coast of the peninsula the winds are parallel to it in South West direction, meeting the NW winds coming from the Atlantic in the Strait.

As regards geostrophic winds, they have only experienced slight variations along the coasts, except for the fact that now they keep close to the Cantabric and Atlantic coasts of the peninsula. There are now South East component winds in the Gibraltar Strait. The medium speed is of 5-10 knots, with the exception of the North Atlantic zone where average winds reach 20 knots.

WEEK FROM JULY 28th TO AUGUST 8th

It is observed that the Atlantic anticyclone now centered to the South of the Azore Islands is now milder, while the Islandian storm which is now approaching through the Irish coast is increasing now. On the other hand, the storm in East Europe has moved towards the South due to another anticyclone with a centre in the Scandinavian peninsula, while the storm in North Africa remains the same.

WEEK FROM AUGUST 9th TO 12th.

The Atlantic anticyclone has moved and is now centered at 42°N 22°W and has been stronger and with a highest influence this week, reaching the Norwegian Coast in the North and the Greek ones in the South of Europe, reaching the Ural Mountains.

The storm in the North is retreating, and the one in Africa maintains its already ordinary place.

With respect to geostrophic winds, they are of a slightly higher intensity with averages of 15 knots on the peninsular Coast, with winds parallel to the Cantabric coast both in France and in the Iberian Peninsula. In Galicia, they have NE components and N component in the South half of the coast. The winds in the Strait are of E component. Thus, the winds predominant this week with respect to the peninsular Coast favour upwelling.

We will now consider three points of the Iberian peninsula on the Atlantic Coast where we will follow the development of geostrophic winds and their Ekman's index.

POINT 42°N9°W

During the first week, July 13th-19th, the winds which appear are increasing their speeds from 5 to 15 knots, with N components at the beginning of the week and NE component at the end, while the Ekman's index increases from 200 to 1200 at the end of the week, all with positive index.

During the week from 20th to 27th there is a decrease in the speed of the winds in the middle of the week with an increase on the 25th and 26th and a fall almost to zero on the 27th.

Similar characteristics appear during the week from July 28th to August 4th, though now with a negative index on August 2nd with ESE component of the wind with a speed of 3 knots giving an index of -158.

During the last week, we can see progressive increases in the speed of the wind from 4 to 10 knots and an index of 300 to 1800 until the 9th, when the mark changes to -2200 and -1500 on the 9th and 10th.

With speeds of up to 12 knots, changing during the last days to values of positive and ENE directions.

POINT 39°N 10°W (in front of the Portuguese Coast)

Here the wind components are mainly North-North East, with maximum speeds on July 13th, 17th, and 25th, with speeds of 9, 10 and 11 knots; and Ekman's constant of 1500, 1900 and 2200 respectively. In August, the peak days would be the 6th and 8th with speeds of 8 and 9 knots and Ekman's indexes of 1300 and 1500 respectively. The days of lowest intensity would be July 27th and 30th and August 9th with speeds of 1, 4 and 3 knots respectively.

POINT 37°N9°W (SW end of the Iberian Peninsula)

In this point, there is a change from strong winds to calm periods every two or three days. The predominant component is from the North, although on 9th, 10th, 11th, and 12th they change to ENE during the first two days with negative Ekman's indexes and ESE the last two days.

The maximums appear on July 15th, 18th, 22th, and 27th and on August 2nd, 3rd, and 12th.

The highest speed reached is of 10 knots and Ekman's index of 1600 on July 17th. The minimum being of 0,4 on the 27th the same month.

We can see in Fig2 an image of the Iberian Peninsula from the IR channel obtained by NOAA-12 in August 12th 1991. On the left we can see the same image after a registration process, in a rectangular format. Both present an overlay coastlines, political boundaries and the main rivers and dams. The image has suffered an enhancement process and we have detected upwelling zones along the Atlantic Coast as we have predicted in our study since July 13th to August 12th.

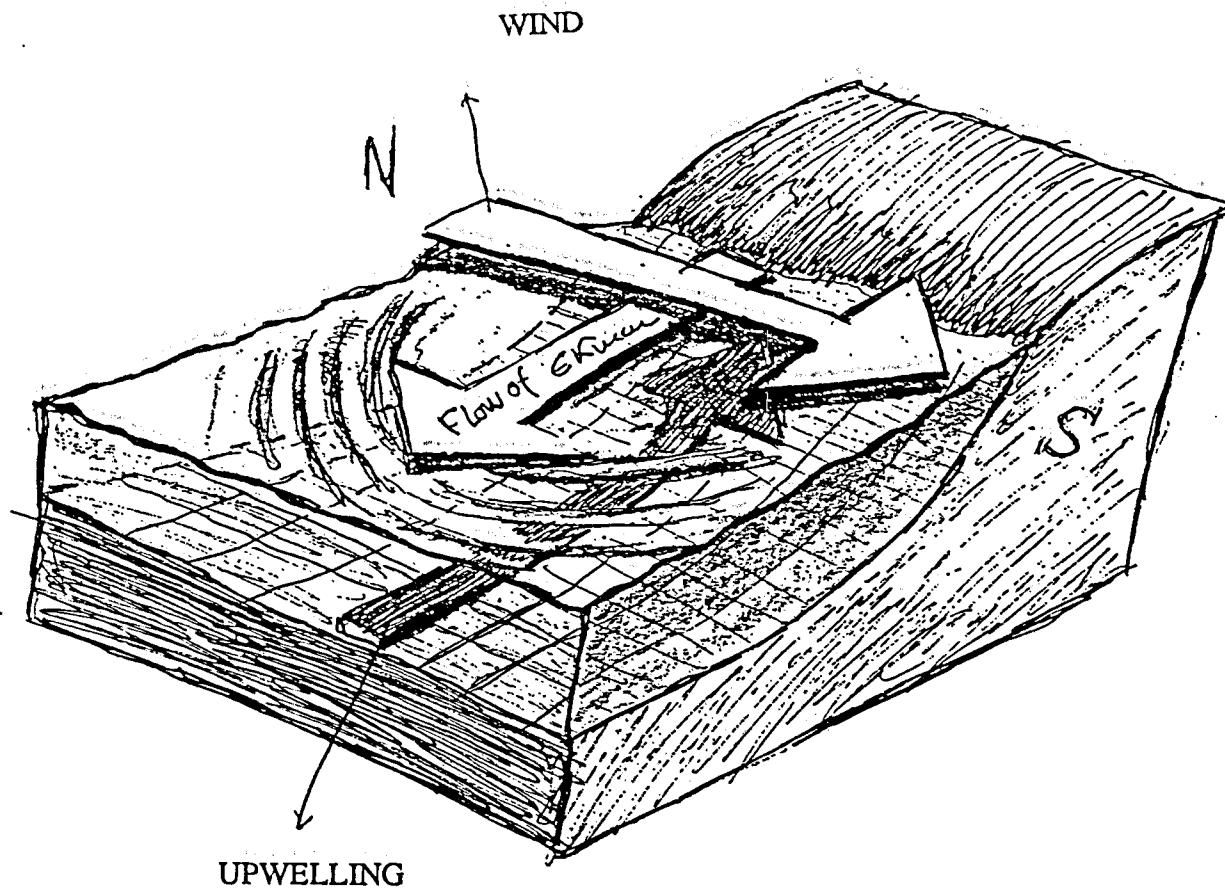
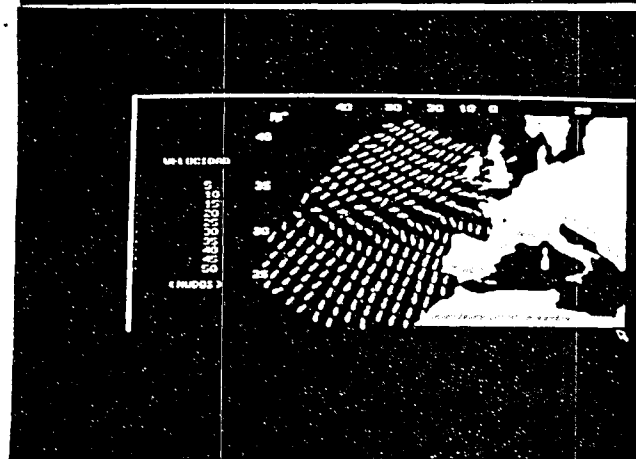
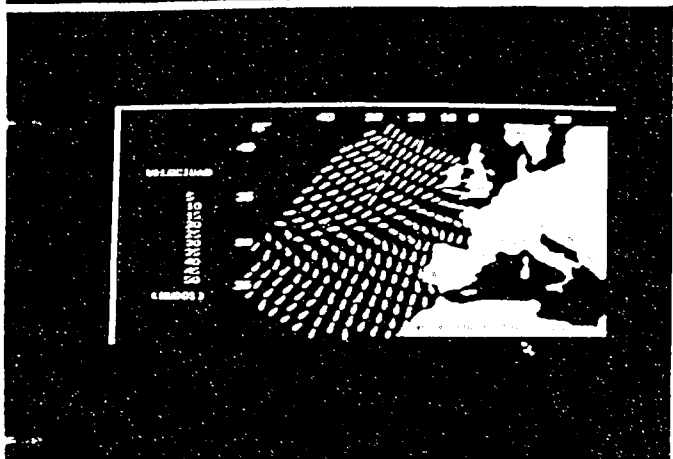
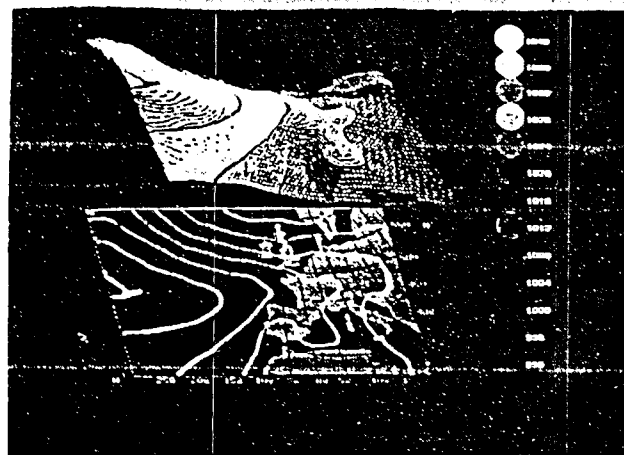
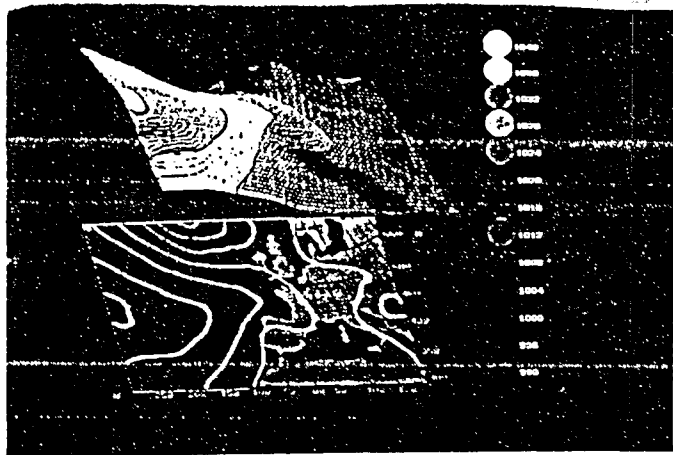


FIG-1

BIBLIOGRAPHY:

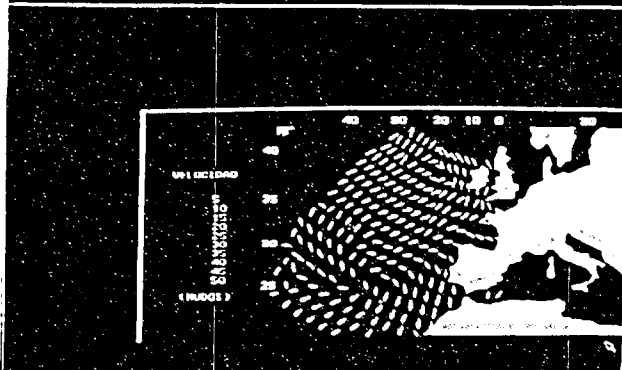
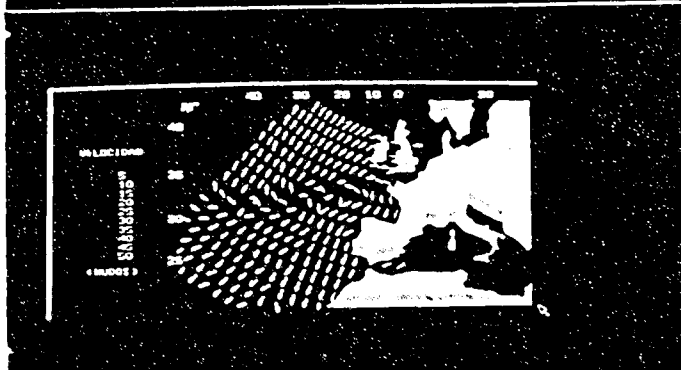
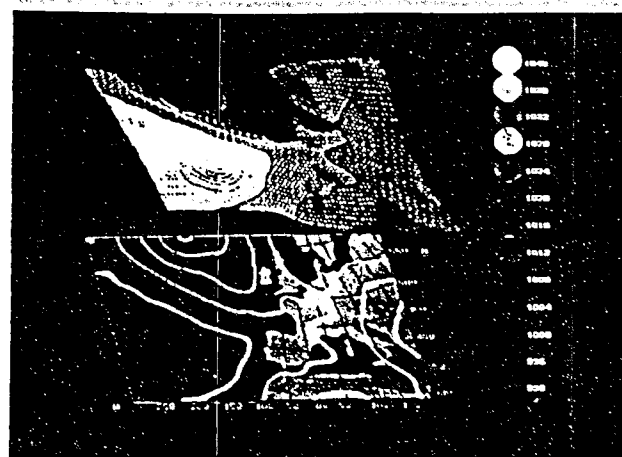
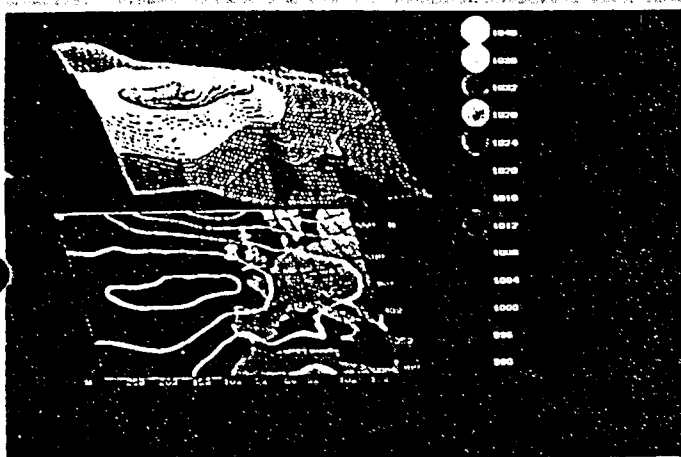
- 1-Trewartha and Horn ."An Introduction to Climate".Quinta edición.
- 2-Ed: David D.Houghton."Applied Meteorology".1985.
- 3-F.Fraga."El Afloramiento costero en la costa atlántica de la península ibérica".
- 4-A.F. de G. Fiúza ,M.E. de Macedo,M.R.Guerreiro."Climatological space and time variation of the Portugese coastal upwelling".Oceanologica acta 1982 - Vol. 5 - Nº 1.
- 5-Andrew Bakun."Global Climate Change and Intensificación of Coastal Ocean Upwelling".Science, Vol 247 Nº 4939, jan 1990 pp 198-201.

- 6-R.Michael Laurs,Heeny S.H. Yuen,and James H. Johnson."Small-Scale movements of albacore,thunnus alalunga,in relation to ocean features as indicated by ultrasonic tracking and oceanographic sampling".Fishery Bulletin.Vol 73 pp 347-355.Laurs,R.M. et Al 1977.
- 7-A.F.G. Fizúa."Application of Satelite remote sensing to fisheries.1990.
- 8-R.Molina."Contribución al estudio del "UPWELLING" frente a la costa noroccidental de la Península Ibérica".
- 9-Blanton , J. O., L.P. Atkinson,F.Fernandez de castillego and a.Lavin Montero."Coastal Upwelling of de Rias Bajas,Galicia,NW Spain.Hidrographic Studies".1982.
- 10-Warren S.Wooster,Andrew Bakun -and Douglas R. McLain."The seasonal upwelling cycle along the eastern boundary of the North Atlantic".Journal of Marine Research.Volume 34,nº 2.1976.
- 11-J.O.Blanton ,K.R. Tenore,F.Castillejo.L.P.Atkinson,F.B.Schwing and A.Lavin."The relationship of upwelling to mussel production in the rias on the western coast of Spain".Journal of Marine Research,45,1987.
- 12.-"Noaa Technical Memorandum NESS 107. Data Extracction and Calibration of TIROS-N/NOAA Radiometers"
Lauritson L., Nelson G., Porto F.W.
- 13.- "Some Marine Applications of Satellite and Airborne Remote Sensing"
Callison R.D., Robinson I.S., Blackburn D.A., Cracknell A.C. Cummings D.L.
UNESCO, July 1989.
- 14.- "Satellite Oceanography. An Introduction for Oceanographers and Remote-Sensing scientists"
Robinson I.S.
Ellis Horwood Limited.
- 15.- "Remote Sensing of the North oest African Upwelling ".Arc N y Kjaer,c
- 16.- "Afloramiento en el Noroeste de la peninsula Ibérica.".Alicia Lavin .Guillermo Diaz del Rio.Instituto Español de Oceanografía.1990.



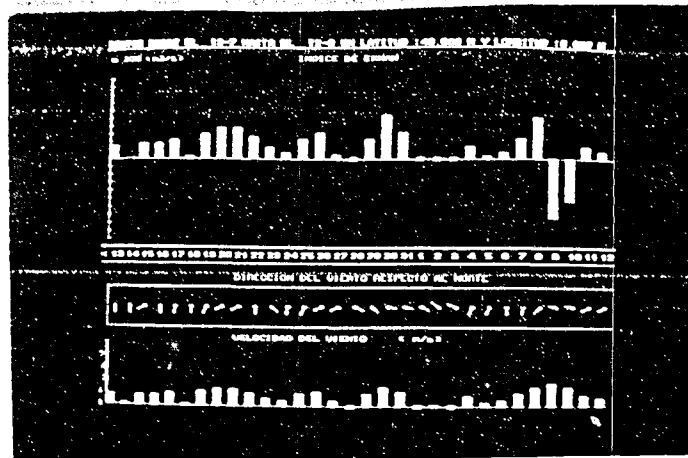
WEEK FROM JULY 13th TO 19th

WEEK FROM JULY 20th TO 27th

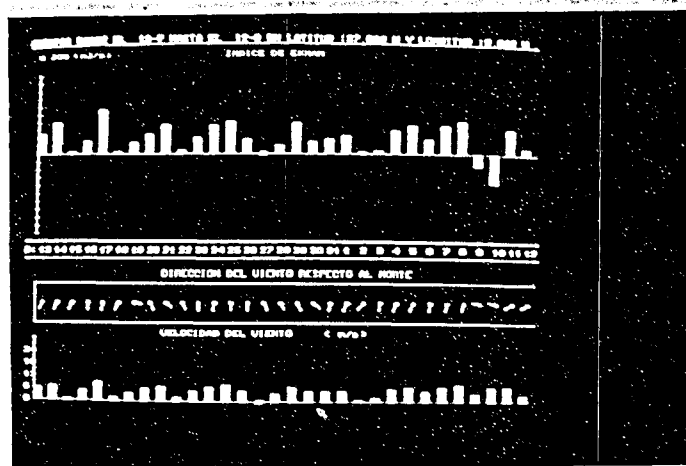


WEEK FROM JULY 28th TO AUGUST 8th

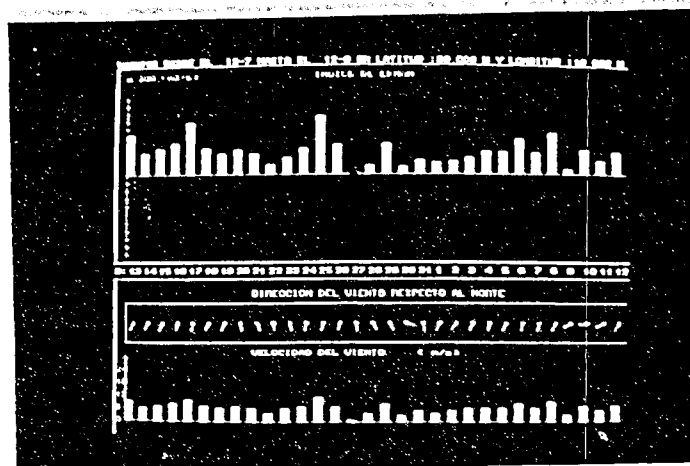
WEEK FROM AUGUST 9th TO 12th.



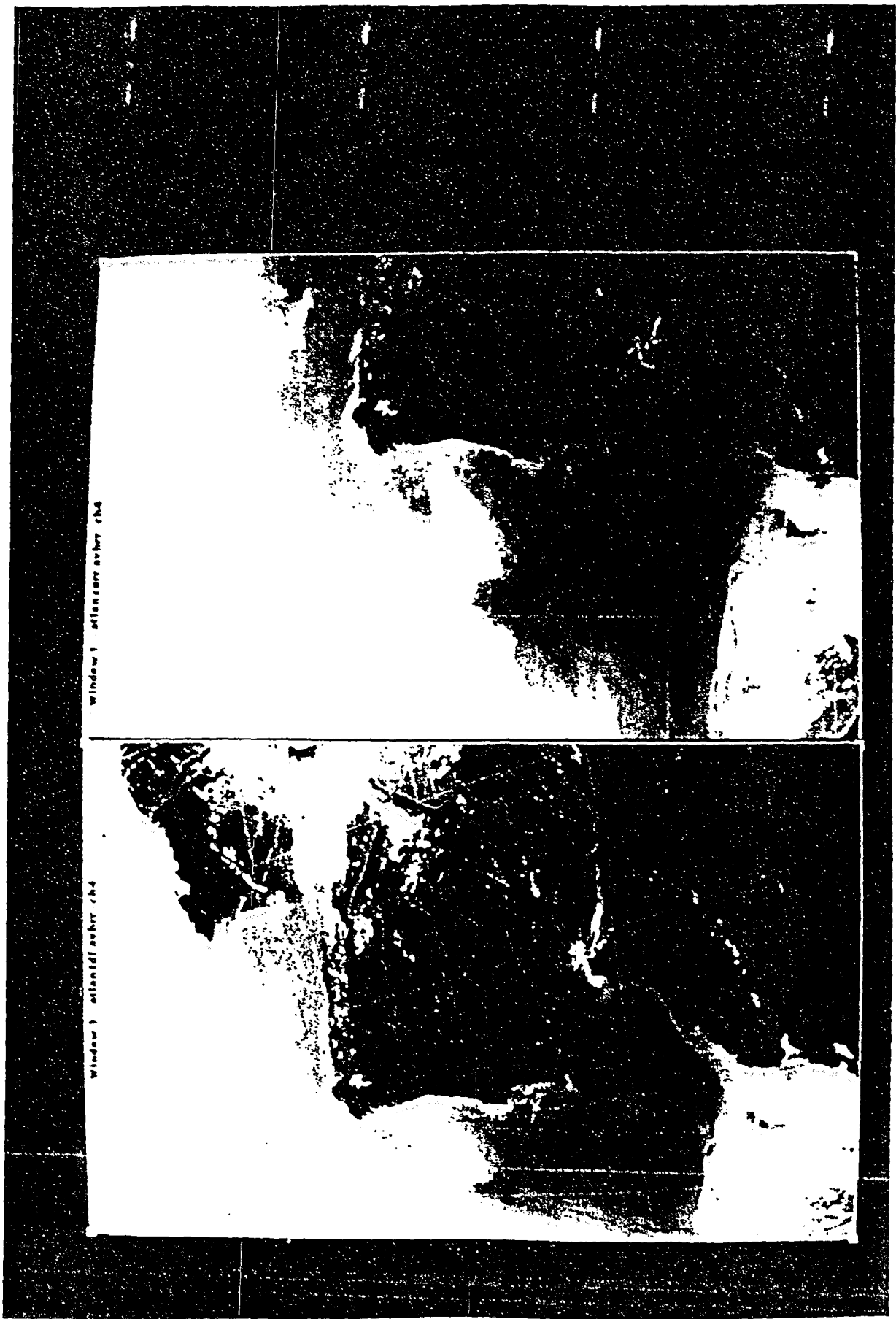
POINT 42°N 9°W



POINT 37°N 9°W (SW end of the Iberian Peninsula)



POINT 39°N 10°W (in front of the Portuguese Coast)



UPWELLING .12th AUGUST 1991
FIG-2